

Hot Pressing of the Silicon Nitride Based Ceramics and Their Mechanical Behavior

D.-S. Park, S.-Y. Lee, H.-D. Kim, W.-S. Choi*, D.-S. Lim* and B.-D. Han*

Ceramic Materials Group, KIMM, 66 Sang Nam Dong, Chang Won 641-010, Korea

*Dept. of Materials Eng., Korea University, Seoul 136-701, Korea

(Received February 14, 1995)

Four kinds of silicon nitride based ceramic materials have been hot pressed. Effect of the sintering additives on the phase transformation, microstructural development and mechanical properties was investigated. While sintering under the same condition produced a big difference among the microstructures of the specimens, they appeared alike if sintered to have a similar α - β phase ratio. The specimen of the stoichiometric α - β sialon composition showed very limited amount of the intergranular glassy phase and a significant degree of the residual stress. It exhibited almost no strength degradation up to 1300°C, and the strength of the specimen degraded more as its composition deviated from the stoichiometry.

Key words: α - β sialon, Phase transformation, Microstructural control, Sintering additives, High temperature strength, Fracture toughness.

I. Introduction

Silicon nitride based ceramics have been extensively studied for the structural applications because they showed good and balanced mechanical properties like hardness, fracture toughness, strength, high temperature strength, thermal shock resistance etc. among the ceramic materials.

It has been well established that the silicon nitride ceramics experience α to β phase transformation during sintering. The phase transformation and the microstructural development of them take place via solution-precipitation process, and the idea of the application of the phase transformation to the microstructural control seems feasible as long as the material showed a sign of changing in phase composition.

One of major advantages of the ceramic materials over the other engineering materials would be the excellent high temperature mechanical properties. The α - β sialon ceramics have been attracting a lot of attention since Ukyo and Wada reported the excellent high temperature strength of the one with a particular stoichiometric composition.¹⁾ They reported higher than 1 GPa strength even at 1400°C. Their TEM micrographs showed that the microstructure consisted of fine α and β sialon grains with small triple points and very limited amount of grain boundary glassy phase. Komeya et al. reported a very impressive high temperature strength of the silicon nitride ceramics containing Y_2O_3 , AlN and HfO_2 .²⁾ They attributed the excellent high temperature strength to the grain boundary crystallization promoted

by HfO_2 . TiN particles have been successfully incorporated in the silicon nitride ceramics and improved the fracture toughness of them.^{3,4)}

In the current study, the silicon nitride ceramics including α - β sialon and the composite containing TiN have been hot pressed. Then, microstructural control via phase transformation was attempted, the microstructures were observed by SEM and TEM and the mechanical properties of the specimens with similar phase ratio (α/β) were measured.

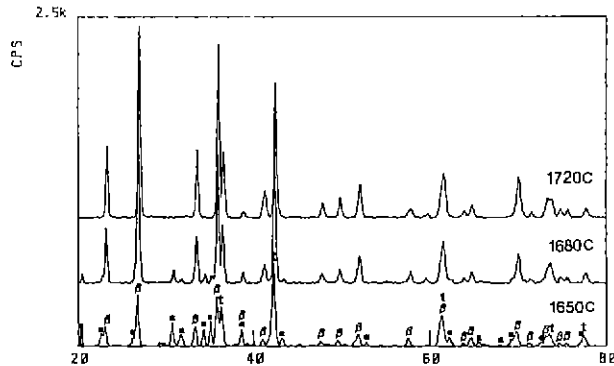
II. Experimental

The powders used for this study were Si_3N_4 (E10), Y_2O_3 (grade 'fine'), AlN (grade 'B'). Si_3N_4 was the product of Ube Co., Japan and the other ceramic powders were the products of H.C.Stark Co., Germany. Four kinds of the silicon nitride-based ceramics were hot pressed. They were labeled A, B, C, and D. Table 1 shows the compositions of the specimens. The powders were ball milled for 72 hours by using ethanol, silicon nitride ball (ϕ 5 mm, SUN 11, Nikkato Co., Japan) and 'Acetal' plastic jar. They were hot pressed in flowing N_2 atmosphere after the usual powder preparation procedure.

In order to measure the α/β phase ratio, the hot pressed specimens were subjected to XRD analysis. The ratio was obtained according to Gazzara and Messier's method.⁵⁾ Hot pressing variables (temperature and time) were chosen to make the phase ratio about 10/90. The specimens with the α/β ratio close to 10/90 have been further employed to study the mechanical properties as well as the

Table 1. Compositions of the Specimens (in wt %)

powder specimen	Si ₃ N ₄	Y ₂ O ₃	AlN	HfO ₂	TiN
A	95	1.9	3.1		
B	93	4	3		
C	90.29	3.88	2.91	2.92	
D	71.61	3.13	2.26		23

**Fig. 1.** The results of XRD analysis for specimen D sintered at (a) 1650°C, (b) 1680°C, and (c) 1720°C; a: α-sialon, b: β-sialon, t: TiN.

microstructures. The specimens for the mechanical testing were finished with 1 mm diamond paste. Vickers hardness of the specimen was obtained by using 500 g load and 15 sec duration. Fracture toughness was obtained according to Evans and Charles' equation after measuring the crack length caused by Vickers indentation under 10 kg load.⁹ Three point flexural strength of the specimens, 3 mm × 4 mm × 34 mm in dimension, was measured with 20 mm span at RT. The high temperature strength measurements at 1400°C were performed with 30 mm span in open air. Ten data and three data were collected for RT and high temperature strength, respectively. Some of the specimens have been annealed at 1250°C for 12 hrs in flowing N₂ and furnace cooled prior to the mechanical testing.

The microstructure was observed by SEM after etching in molten NaOH-KOH salt. TEM specimens were prepared according to the standard procedure, i.e. grinding-dimpling-ion milling. The perforated 3 mm disk after ion milling was carbon-coated to prevent charging. Jeol 2000 CX TEM equipped with EDS was employed for the observation.

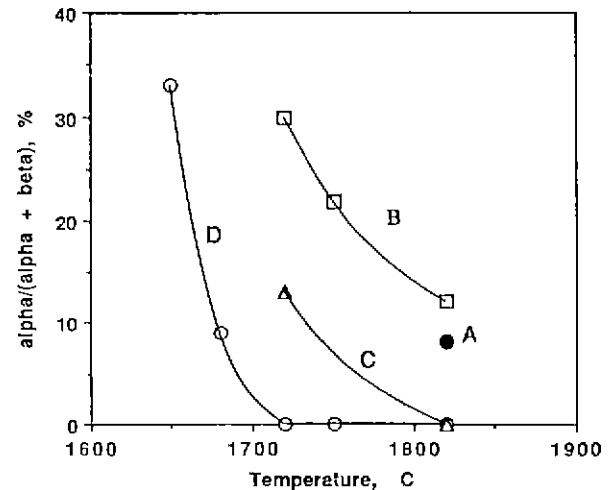
III. Results and Discussions

1. Phase transformation during hot pressing.

The phase transformation of the silicon nitride ceramics from α to β depends on the chemical composition as well as the sintering temperature.⁷ Fig. 1 shows the XRD results obtained from specimen D at various hot pressing temperatures. As expected, the phase transformation

Table 2. Hot Pressing Conditions vs. α/β Phase Ratio

specimen	H.P. condition T(°C)/time(hr)/P(MPa)	α/β
A	1820/1/30	10/90
B	1820/1/30	12/88
C	1720/1/30	13/87
D	1680/1/30	9/91

**Fig. 2.** Variation of α/(α+β) ratio according to the hot pressing temperature; the specimens showed very different phase transformation behaviors from one another.

from α to β heavily depended on the temperature. In case of specimen D, the α/β ratio was about 1/2 at 1650°C and it dropped very rapidly down to 1/9 only at 1680°C. No α phase was detected after hot pressing for 1.5 hrs at 1720°C. The difference of chemical compositions of the four specimens would affect the nature (chemical characteristics, viscosity and etc.) and the amount of the liquid present. Therefore, the phase transformation during hot pressing was expected to be different from each other. Fig. 2 shows the variation of the α/(α+β) ratio as a function of hot pressing temperature. The specimens showed a different phase transformation behavior; the phase transformation of specimen A and B occurred more sluggishly than the others. The chemical nature of the liquid present at sintering temperature would be critical to the phase transformation of the silicon nitride based ceramics. Kang et al. reported the phase transformation from α to β sialon taking place by the reaction between sintered α sialon and the liquid stabilizing β sialon.⁸ Mandal and Thompson reported the reversible α-β sialon transformation in heat-treated sialon ceramics and more α sialon forming at high temperature.⁹ Ukyo et al. also reported more α sialon at high temperature.¹⁰ These reports are quite different from the result of the current study which is showing the decreasing amount of α sialon as temperature increased. Ukyo et al. suggested that there were two kinds of α sialon; unstable and stable.¹¹ According to

them, the α sialon obtained in this study must have been unstable and would disappear if kept at high temperature. Therefore, the liquid surrounding the α phase grain was stabilizing β phase in this study. It is amazing that specimen B containing excess Y_2O_3 to the stoichiometric composition showed a similar $\alpha/(\alpha+\beta)$ ratio to what specimen A of stoichiometric composition did after hot pressing at $1820^\circ C$; this was due to the liquid of different chemistry and, therefore, of different reactivity with the α phase. Specimen C containing HfO_2 in addition to Y_2O_3 and AlN showed a faster phase transformation than A or B. This implies that a part of HfO_2 was involved in the liquid at the hot pressing temperature, and changed the chemistry. This change in the chemistry of the liquid triggered faster phase transformation from α to β . Actually, there was no α sialon detected for specimen C hot pressed at $1820^\circ C$, which was quite different from the XRD result of specimens A and B. HfO_2 was incorporated to facilitate the crystallization of the grain boundary phase by acting as the nuclei⁸. Specimen C was annealed at $1250^\circ C$ for 12 hrs in N_2 atmosphere, but there was no

other crystalline phase detected by XRD except α and β sialon. Heat treatment might need an optimization.

Specimen D was a composite material containing 15 v/o TiN. TiN has a surface oxide like other non-oxide ceramic powders. The surface oxide was thought to be involved in and change the nature of the liquid. The specimen exhibited the fastest phase transformation as shown in Fig. 2. From the XRD results, the hot pressing temperature and was determined to make the α/β ratio close to 10/90. The conditions are shown in table 2.

2. Microstructural analysis

The specimens used for the microstructural analysis and the mechanical property measurements were fully dense (relative density > 99.4% of theoretical density). Fig. 3 shows the micrographs of the specimens A, B, C and D with α/β ratio about 10/90. Even though C appeared to have slightly finer grains, it can be well understood that the microstructures of the specimens were very close to each other considering that the micrographs were taken under high magnification (X10,000).

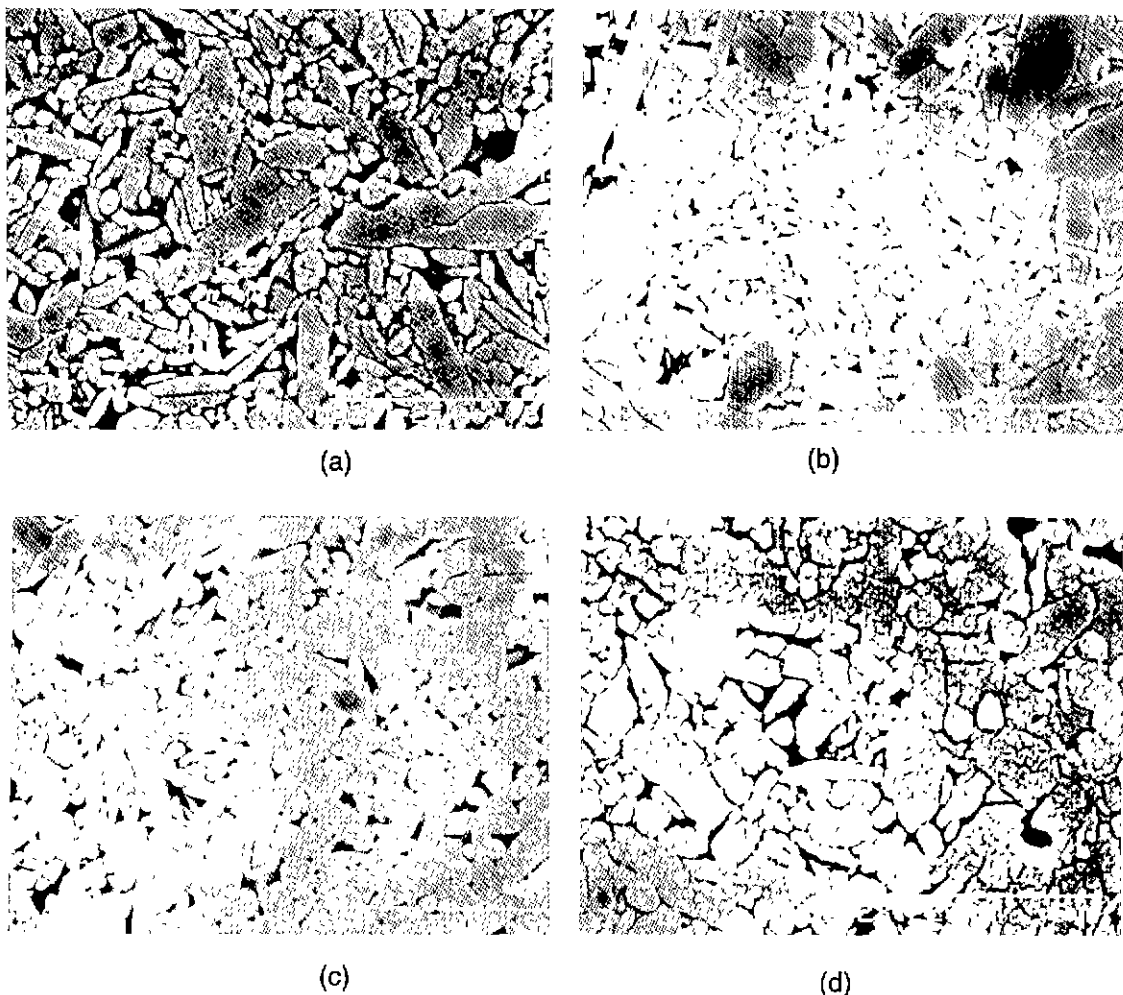


Fig. 3. SEM micrographs of the specimens with α/β of about 10/90; (a) A, (b) B, (c) C and (d) D showing similar matrix grain sizes despite the big difference in the hot pressing temperatures.

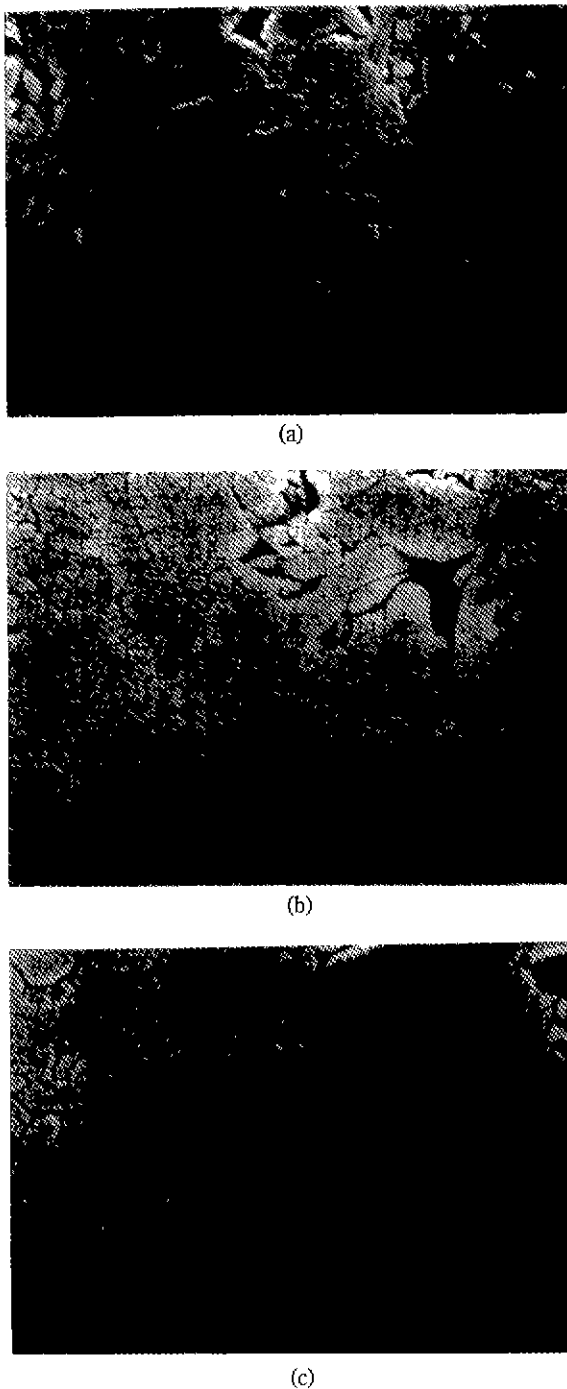


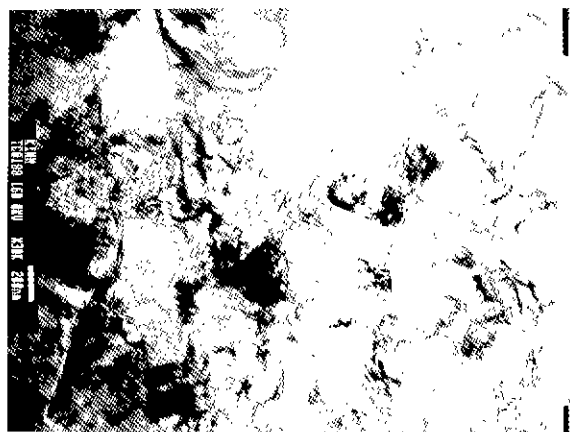
Fig. 4. SEM micrographs of the specimens hot pressed under the same condition: (a) B, (b) C and (c) D, showing the big difference in the matrix grain sizes.

For comparison specimen C and D were hot pressed at 1820°C for 1hr as specimens A and B were, and the resulting microstructure are shown in Fig. 4. Much bigger grain sizes were observed for specimen C and D than for B. This proves that the phase transformation of α to β sialon can be used for better microstructural control of the ceramic. Depending on the microchemical composition, each specimen was influenced by the sintering tem-

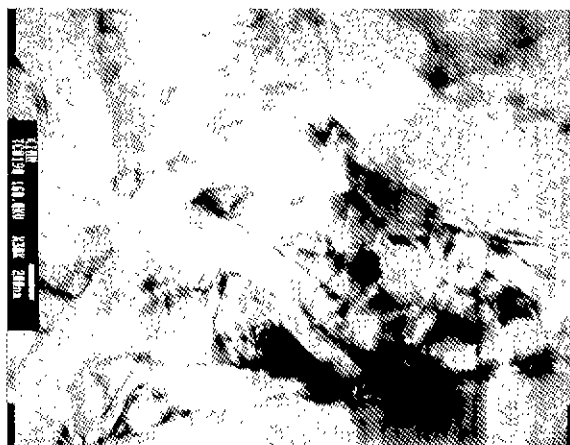
perature and time in different ways. In other words, even if the same sintering conditions were applied, each specimen showed its own phase transformation behavior and microstructural development. From the current study, the phase transformation of a specimen was found to be in close relationship with the microstructural development, which was observed from the similar microstructures of the specimens with similar α/β phase ratio. It is the degree of heat to which each material system felt that dictated both the phase transformation and grain growth.

Fig. 5 shows the TEM micrographs of specimens A, B and C. Specimen A contained a significant amount of residual stress which was expressed by the complex fringes over the entire field of view. This also strongly suggests that the specimen contained a very limited amount of the intergranular stress-relieving layer. Specimen B had excess Y_2O_3 and its TEM micrograph showed that it had the stress-relieving intergranular phase. The micrograph does not exhibit the extensive complex fringes and the very 'clean' image, expressing a very low level of the residual stress present, if any. Also, the small grains of B exhibited more elongated shapes (higher aspect ratio) than those of A. More liquid at the sintering temperature facilitated the anisotropic growth of the grains in B compared with the restrained grain growth in A. Therefore, the increased amount of the liquid can explain the absence of the complex fringes as well as the higher aspect ratio of the smaller grains of B.

Specimen C exhibited larger amount of the liquid phase than B as shown in Fig. 5 (c). The matrix consisted of the large elongated grains and the very small equiaxial grains. In spite of the larger amount of liquid in C than in B, the former showed equiaxial grains smaller than those of the latter. This was possibly due to the lower sintering temperature and slightly higher content of a phase of C. Also, HfO_2 particles appeared as dark spots scattered on the micrograph, some of which were entrapped in much bigger matrix grains. There were two purposes of adding HfO_2 to specimen C; the first was the possible nucleation sites for the crystallization of the grain boundary glassy phase and the second was the possible sink for the excess Y_2O_3 to make Y_2O_3 stabilized HfO_2 . Fig. 6 (a) shows the phase next to the HfO_2 particle. The inset pattern reveals that the region was amorphous. Therefore, HfO_2 did not help the expected crystallization of the grain boundary glassy phase. Since one heat treatment schedule was performed, it might need further efforts for optimization. Fig. 6 (b) exhibits the triple point. EDS result on the area revealed that it was composed of Y, Si, Al, O and N and no Hf was detected. It means that HfO_2 particles precipitated back from the liquid during cooling and left the Hf-free glass. Also, Fig. 6 (c) showed the HfO_2 particle entrapped in the bigger matrix grain. Therefore, some of the HfO_2 particles did not dissolve in the liquid phase during sintering and not all of



(a)



(b)



(c)

Fig. 5. TEM micrographs of specimens A, B and C: (a) A showing the extensive fringe pattern implying a significant amount of residual stress present, (b) B showing much 'clean' image and more elongated grains than A, (c) C showing richness of the liquid and HfO_2 particles scattered over the specimen

them would have reacted with the liquid. The EDS analysis on the particle revealed no Y, which means that Y_2O_3 did not dissolve in HfO_2 to stabilize it.

3. Mechanical properties.

Fig. 7 shows the results of microhardness and K_{IC} measurements. Vickers microhardness values of the specimens were similar to one another and in the range of 16-17 GPa. The K_{IC} values of specimens A, B, C and D were $5.64 \text{ MPa}\sqrt{\text{m}}$, $6.13 \text{ MPa}\sqrt{\text{m}}$, $6.0 \text{ MPa}\sqrt{\text{m}}$ and $6.45 \text{ MPa}\sqrt{\text{m}}$, respectively. They were consistent with the expectation from the microstructural observation; Specimens B and C provided the weak grain boundary for crack propagation and the crack detoured around the grains to improve K_{IC} ; in contrast, there was a very limited amount of weak grain boundary in A and the crack would cut straight the grains to make K_{IC} lower. The existence of TiN was contributed to improving K_{IC} as expected.

Fig. 8 exhibits the three point flexural strength of the specimens. The strength was measured at RT and at 1300°C . At RT, specimen C exhibited the highest strength of 1200 MPa and A, B and D showed 1106 MPa, 945 MPa and 1028 MPa, respectively. As well known, the microstructure has a strong influence upon the strength of the ceramic materials. But the specimens of the current study showed quite different values in strength in spite of the similar microstructures. The reason for higher strength of specimen A than that of specimen B was closely related to the residual stress as mentioned by Sun et al.¹⁹ The residual stress was already mentioned based on TEM micrograph (Fig. 5) of specimen A. At 1300°C , the strength of the specimen decreased as its composition deviated from the stoichiometry. Specimen A of the stoichiometric composition was shown to have a very limited amount of the glassy phase and it suffered almost no strength degradation even at 1300°C . Considering that the high temperature flexural strength was obtained with 30 mm span while the RT strength was with 20 mm span, 1075 MPa at 1300°C was almost the same as the value obtained at RT. Specimen B exhibited 820 MPa at 1300°C which was about 130 MPa lower than the strength at RT. Specimen C showing the highest strength at RT suffered about 500 MPa decrease at 1300°C . The decrease was expected from the TEM micrograph (Fig. 5(c)) which disclosed a lot of glassy phase present in specimen C and HfO_2 did not help crystallization of it.

However, the high temperature strength of specimens A, B and C was higher than that of the silicon nitride sintered with Y_2O_3 and Al_2O_3 . Fig. 9 shows the fracture surface of specimen C after the high temperature strength measurement. It was covered with a glassy layer except the small area at the fracture origin shown in Fig. 9(b). While Fig. 5(c) and the high temperature strength degradation supported the fact that a lot of liquid phase was present at hot pressing temperature. The liquid did not wet the grains well enough and the non-sintered area was left to be the fracture origin.

Specimen D showed the lowest high temperature strength; 300 MPa at 1300°C . TiN, when incorporated in

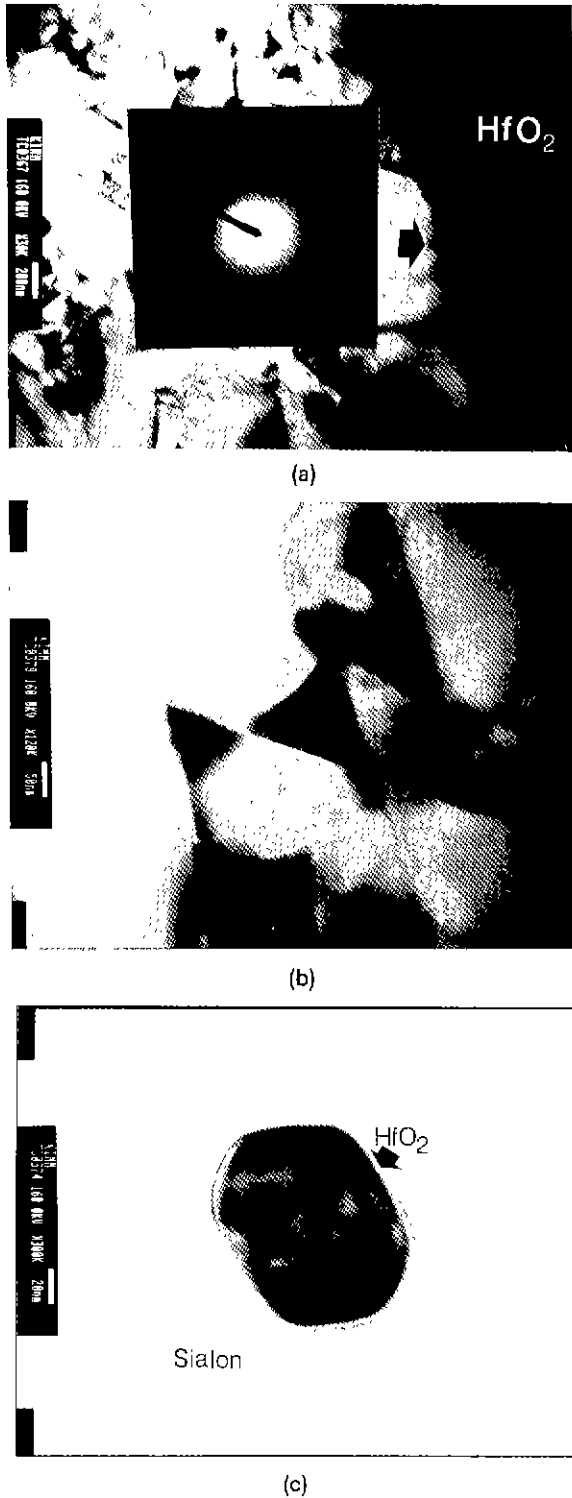


Fig. 6. TEM micrographs of specimen C; (a) amorphous intergranular region (inset pattern) next to HfO_2 particle (large dark contrast), (b) triple point region containing no Hf and (c) HfO_2 particle entrapped in sialon grain showing it was inert to the liquid at the pressing temperature.

Si_3N_4 based ceramics, was reported to badly deteriorate not only the oxidation resistance of the matrix but also the high temperature strength.⁵⁷ The observed low

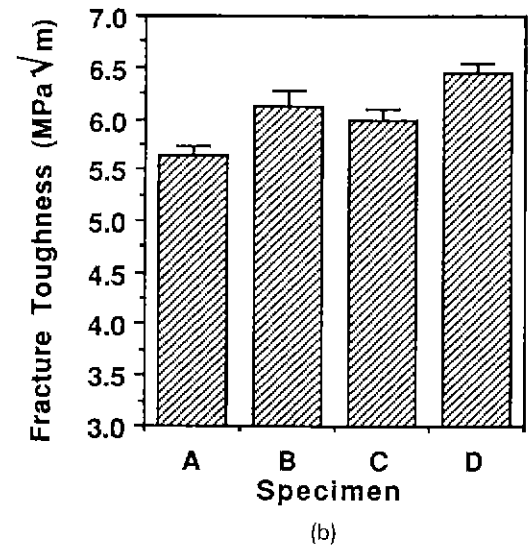
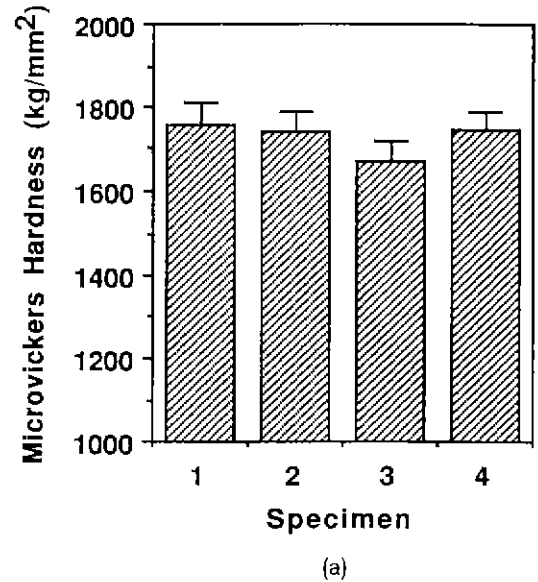


Fig. 7. Vickers microhardness (a) and fracture toughness (b) of the specimens; hardness was in the range of 16-17GPa and fracture toughness showed the dependence upon the chemical composition and the microstructure.

strength at 1300°C can be interpreted as a result of the bad oxidation resistance which deteriorated the surface roughness and the low viscosity of the liquid including TiO_2 . Fig. 10 shows the fracture surfaces of specimens A and D. Both of them exhibited extensive oxidation product covering the surface. While specimen A was covered with the layer containing many tiny (smaller than 1 mm dia.) pores, specimen D was with the layer containing large particles (about 3 mm big) and big pores. Apart from the surface appearance, the contact between the oxidation product layer and the substrate was very loose and the layer was easily wiped off by touching. Five of each specimens were annealed for 12hrs at 1250°C in flowing N_2 and tested for the flexural strength at RT. There was little change of the strength occurred to speci-

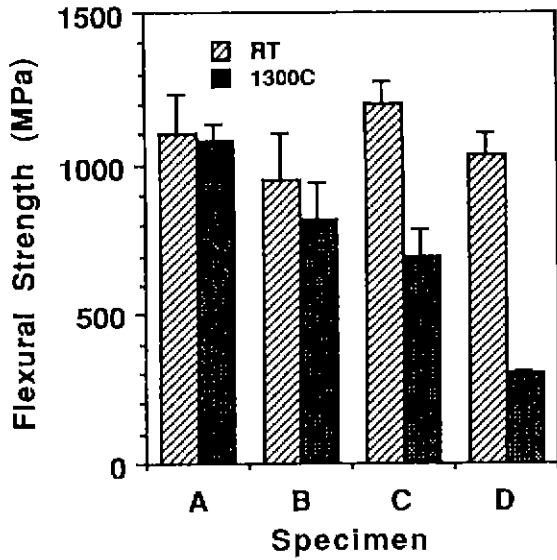
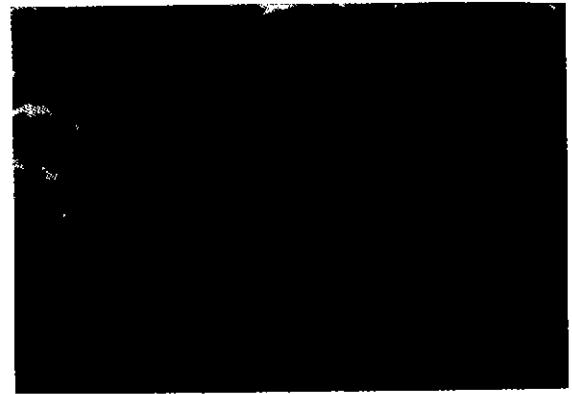
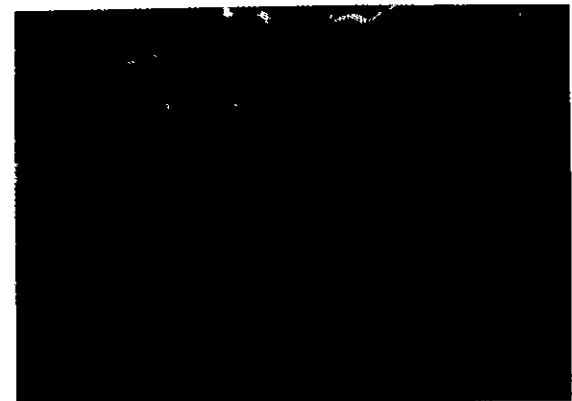


Fig. 8. Three point flexural strength of the specimens at RT and 1300°C; span for strength was 20 mm and for 1300°C was 30 mm, measurements conducted in open air and crosshead speed was 0.5 mm/min. Note the high temperature strength retention of specimen A as well as the effect of the chemical composition deviating from the stoichiometry of the high temperature strength degradation.

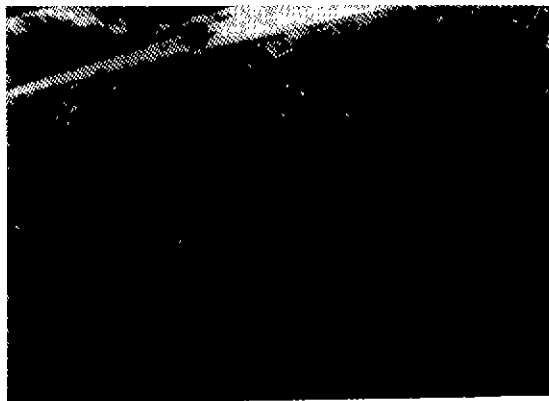


(a)



(b)

Fig. 10. Fracture surface of (a) specimen A and (b) specimen D after the three point bend test at 1300°C; the surface was covered with an oxide layer containing either tiny pores (a) or big grains and pores (b).



(a)



(b)

Fig. 9. SEM micrographs of the fractured surface of specimen C tested at 1300°C; (a) at a low mag. showing hackles pointing to the fracture origin and (b) an enlarged view of the fracture origin exhibiting non-sintered area.

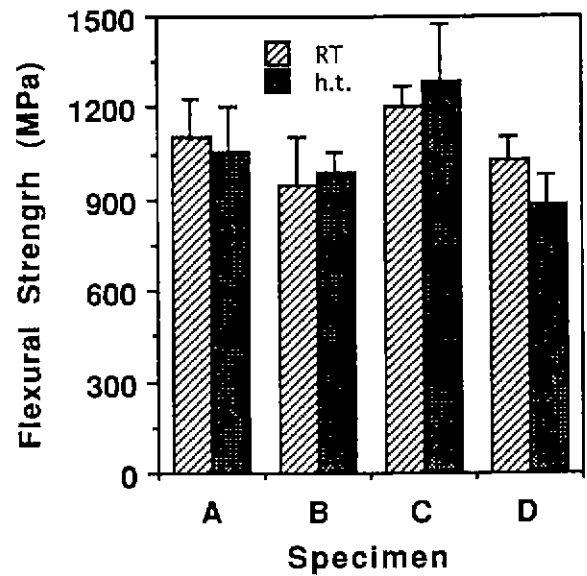


Fig. 11. Three point flexural strength measurements before and after the heat treatment at 1250°C for 12hrs in N₂; note a significant strength degradation of specimen D.



(a)



(b)

Fig. 12. Optical micrographs of specimen D (a) before and (b) after the heat treatment at 1250°C for 12hrs in flowing, N₂ gas environment; note TiN particles fell off during the heat treatment cycle and caused the strength degradation measured in fig. 11.

mens A, B and C. Specimen D experienced a significant amount of strength reduction, about 140MPa, caused by the heat treatment (Fig. 11). The strength decrease can be explained by Fig. 12 which shows the TiN particles (bright contrast spots in (a)) fell off the specimen and left the surface flaws (dark contrast spots in (b)). These surface flaws were the causes for the strength degradation after the heat treatment. Metal nitride ceramic particles including TiN have been considered as a toughening agent for Si₃N₄ based ceramics by many investigators.^{3,4,6,13,14} They might be contributed to the reinforcement at RT. Woydt et al. reported a lower friction coefficient and wear rate for the Si₃N₄-TiN composite than for the monolithic silicon nitride.¹⁵ However, the particulate composites like D were very vulnerable to the exposure to high temperature. They suffered from severe oxidation and strength degradation. Also, they exhibited the strength degradation after a simple heat treatment even in N₂. Therefore, silicon nitride ceramics containing TiN are thought to perform well as a structural ceramic material at low temperature, but there needs a precaution for applying them for the high temperature purposes even in

inert atmosphere.

IV. Conclusions

The following conclusion were reached.

1. The α to β phase transformation of the silicon nitride based ceramics critically depended on the chemical species involved in the ceramics and the composite material containing TiN showed the fastest transformation among the specimens studied.
2. Microstructures of the silicon nitride based ceramics were controlled better by taking advantage of the phase transformation than by sintering conditions.
3. Specimen A with stoichiometric α - β sialon composition showed very limited amount of the intergranular glassy phase and significant amount of the residual stress present, and excess Y₂O₃ in specimen B formed enough intergranular glassy phase to relieve the residual stress.
4. Some of HfO₂ added to specimen C was not involved in and stayed inert to the liquid at the hot pressing temperature and it neither worked as nuclei for the crystallization of the grain boundary phase nor accommodated the excess Y₂O₃.
5. Specimen A of the stoichiometric composition for α - β sialon showed almost no strength degradation up to 1300°C and the specimens exhibited more strength degradation as they deviated from the stoichiometry as expected from the microstructural analysis.
6. TiN was helpful in improving K_{IC} at RT of the ceramic, but it caused a significant strength degradation at 1300°C and after heat treatment at 1250°C in flowing N₂.

Acknowledgement

This work was supported by Ministry of Science and Technology. Authors appreciate Mr. Y. Kim for TEM operation. They also would like to express thankfulness to professor K. Komeya at Yokohama National Univ., Japan for the advice and Dr. T. Ekstrom at University of Stockholm, Sweden for the fruitful discussions.

References

1. Y. Ukyo and S. Wada, "High Strength Si₃N₄ Ceramics," *Nippon Seramikkusu Kyokai Ghujutsu Ronbunshi*, **78** [8], 872-874 (1989).
2. K. Komeya, M. Komatsu, T. Kameda, Y. Goto, Y. Goto and A. Tsuge, "High-Strength Silicon Nitride Ceramics Obtained by Grain-Boundary Crystallization," *J. Mater. Sci.*, **26**, 5513-5516 (1991).
3. T. Ekstrom and P.-O. Olsson, " β -Sialon Ceramics with TiN Particle Inclusions," *J. Euro. Ceram. Soc.*, **13**, 551-59 (1994)
4. T. Nagaoka, M. Yasuoka, K. Hirao and S. Kanzaki, "Effects of TiN Particle Size on Mechanical Properties of

- Si₃N₄/TiN Particulate Composites," *J. Ceram. Soc., Jpn.*, **100** [4], 617-620 (1992).
5. C. P. Gazzara and D. R. Messier, "Determination of Phase Content of Si₃N₄ by X-Ray Diffraction Analysis," *Am. Ceram. Soc. Bull.*, **56** [9], 777-780 (1997).
 6. A. G. Evans and E. A. Charles, "Fracture Toughness Determined by Indentation," *J. Am. Ceram. Soc.*, **58** [7-8], 371-372 (1976).
 7. G. N. Babini, A. Bellosi and P. Vincenzini, "Hot Pressing of Silicon Nitride with Ceria Additions," *Ceram. Int.*, **6**, 91-98 (1980).
 8. S.-J. L. Kang, S.-M. Han, D.-D. Lee and D.N. Yoon, "α-β Phase Transition and Grain Morphology in Y-Si-Al-O-N System," *MRS Int. Mth. of Adv. Mater.*, **5**, 63-67 (1989).
 9. H. Mandal and D.P. Thompson, "Reversible α-β Sialon Transformation in Heat Treated Sialon Ceramics," *J. Euro. Ceram. Soc.*, **12**, 421-429 (1994).
 10. Y. Ukyo and S. Wada, "Sintering Reaction in the System Si₃N₄-Y₂O₃-AlN," *J. Ceram. Soc. Jpn.*, **102** [7], 623-626 (1994).
 11. Y. Ukyo, N. Sugiyama and S. Wada, "Thermal Stability of Y-α-Sialon Prepared from Si₃N₄-Y₂O₃-AlN," *J. Ceram. Soc. Jpn.*, **102** [8], 713-717 (1994).
 12. S. Wada, "Processing and Properties of the Self-Reinforced Ceramics," *New Ceramics*, **7**[7], 87-100 (1994)
 13. D.-S. park, H.-D. Kim, S.-Y. Lee and S. Kim, "Gas Pressure Sintering of Si₃N₄-Base Particulate Composites and Their Wear Behavior," *Key Eng. Mater.*, **89-91**, 439-444 (1994).
 14. Y.G. Gogotsi, G. Grathwohl and G.E. Khmenko, "Structural Evolution of Silicon Nitride-Titanium Nitride Composites During High-Temperature Creep," *Key Eng. Mater.*, **89-91**, 659-664 (1994).
 15. M. Woydt, A. Skopp and K.-H. Habig, "Dry Friction and Wear of Self-mated Sliding Couples of SiC-TiC and Si₃N₄-TiN," *Wear*, **148**, 377-384 (1991).